Synthesis and Characterization of Poly(3-octylthiophene)/ Single Wall Carbon Nanotube Composites for Photovoltaic Applications

Hee Jin Kim,[1] Raushan B. Koizhaiganova,[1] Mohammad Rezaul Karim,[2] Gang Ho Lee,[1] Thiagarajan Vasudevan,[1] Mu Sang Lee[1]

[1]*Department of Chemistry, Teachers college, Kyungpook National University, Daegu 702-701, South Korea*
[2]*Center of Excellence for Research in Engineering Materials, College of Engineering, King Saud University, Riyadh 11421, Saudi Arabia*

Received 22 July 2009; accepted 28 February 2010
DOI 10.1002/app.32436
Published online 3 June 2010 in Wiley InterScience (www.interscience.wiley.com).

ABSTRACT: *In situ* polymerization of P3OT with SWCNT is carried out in the presence of a $FeCl_3$ oxidant in a chloroform medium. The characterization of the composites is performed with FTIR, Raman, ^{1}H-NMR, UV–Vis, PL spectroscopy, XRD, SEM, TEM, and conductivity measurements. The change (if any) in C=C symmetric and antisymmetric stretching frequencies in FTIR, the shift in G band frequencies in Raman, any alterations in λ_{max} of UV–Vis and PL spectroscopic measurements are monitored with SWCNT loading in the polymer matrix. ^{1}H-NMR confirms the wrapping of the polymer on to the SWCNT indicating lack of mobility. The work function values and the optical band gap values also support this view. The *in situ* polymerization procedure of the donor polymer molecules and the acceptor carbon nanotubes has resulted in enhanced dispersibility and stability of the composites in organic solvents. However, the principal focus of the study is to understand the interaction between the polymer and the SWCNTs, as the interface plays an important role in its application in the photovoltaic cells. © 2010 Wiley Periodicals, Inc. J Appl Polym Sci 118: 1386–1394, 2010

Key words: conducting polymers; fillers; nanocomposites

INTRODUCTION

In polymer-photovoltaic devices, fullerenes,[1,2] nanoparticles,[3,4] carbon nanotubes,[5–8] and conjugated polymers with high electron affinity[9–11] are being used to hybrid with semiconducting polymers like polythiophene or poly(*p*-phenylene vinylene) (PPV).[12]

Since the first report of a polymer/SWCNT photovoltaic device in 2002, it has increased interest in such type of composites is evident from the very large number of publications on polythiophene (PT)/carbon nanotube (CNT) composites that are appearing periodically with more and more innovative ideas for the creation of an effective interface between the PT and CNT. Electron-hole pairs are generated at the interface of the polymer and CNTs upon illumination. The carbon nanotubes serve as electron traps as they have more electron affinities than the conjugate polymers. SWCNT are more stable in air than fullerenes and are also much cheaper. They are also excellent electrical conductors and they eliminate the charge transport barriers of hopping between acceptor molecules. The general methods to prepare polymer-CNT composites are:

1. Ultrasonication of CNT or surface functionalized CNT in presence of matrix polymers
2. The *in situ* polymerization of monomers in the presence of CNT;
3. Polymerization of the matrix polymer from the surface of the nanotubes.

In these cases a nanohybrid/nanoconjugate is to be formed depending upon the interaction between the polymer and the CNT. In addition to intensive and intimate interfaces being formed between them, there is the additional advantage of easy solubilization in many organic solvents.

Considering all these aspects, recently, the direct of polymerization of monomers in a CNT–dispersed medium through functionalization/nonfunctionalization of CNT has drawn great attention to prepare polymer-wrapped CNT.[13–20] The supramolecular approach of noncovalent modifications of CNT seems attractive as it will not disrupt the extended π-networks and open up the possibilities of being

Correspondence to: M. R. Karim (mkarim@ksu.edu.sa) or M. S. Lee (mslee@knu.ac.kr).

Contract grant sponsor: Korea Research Foundation; contract grant number: KRF-2006-005-J02401.

able to organize the nanotubes in the ordered polymer matrix. In this direction, *in situ* synthesis and characterization of soluble poly(3-octylthiophene)/SWCNT composites for solar cell applications has been attempted as a first report. The morphology, microstructure, and physical properties, including thermal and electrical aspects, are discussed in detail. A close look at the interface between the polymer and SWCNT is made out to understand the nature of the interaction between them.

EXPERIMENTAL SECTION

Preparation of the nanocomposite/polymer

SWCNT (AP-grade, diameter: 1–1.2 nm, length: 2–20 μm) supplied by the Iljin Nanotech Co., South Korea was used in the as procured form. 3-Octylthiophene (3OT) monomer (97%), chloroform, iron (III) chloride anhydrous (oxidant), and other organic solvents purchased from Aldrich as reagent grade were used without further purification.

A typical *in situ* chemical oxidative polymerization for the 3OT and SWCNT-3OT was carried out. The synthesis for the composite consists of the following steps: 100 mL of $CHCl_3$ solution containing SWCNT (varying amounts to get 1, 5, 10, and 20 wt % with respect to the monomer weight) was added to a 250 mL double-neck, round bottomed flask carrying a magnetic Teflon-coated stirrer. The mixture was sonicated for 1 h at room temperature to disperse the SWCNT. $FeCl_3$ (2 g) in 100 mL $CHCl_3$ solution was added to the above solution and further sonicated for 30 min. 3OT monomer (0.5 mL) in a 25 mL $CHCl_3$ solution was taken in a condenser and added drop wise to the SWCNT and $FeCl_3$ solution with constant stirring. The reaction mixture was stirred for an additional 24 h under the same conditions. The resultant SWCNT-P3OT composite was precipitated in methanol, filtered using a Buchner funnel and then carefully washed several times with methanol, 0.1*M* HCl, distilled water, and acetone. The obtained brownish black powder was dried under a vacuum dryer at room temperature for 24 h. The polymer was synthesized following the same procedure.

Characterizations

Gel permeation chromatography Waters, Alliance GPCV 2000 with Waters 2414 Refractive Index Detector and a column of Ultrastyragel linear P/N 10,681 from Waters was used to measure the molecular weight distribution relative to polystyrene standards. The calibration curve was determined by use of 10 MW standards from MW 2000 to 10^6. The carrier solvent used was tetrahydrofuran at a flow rate of 1 mL/min.

Molecular structure of the obtained 3-octylthiophene product and composite (20 wt %) were identified by nuclear magnetic resonance (NMR ^1H) using $CDCl_3$ as a solvent in a Varian Unity INOVA equipment with a resonance frequency of 500 MHz.

The X-ray diffractions were measured using a PANalytical (Netherland) Model – X-ray diffractometer. The X-ray beam was Cu Kα ($\lambda = 0.1541$ nm) radiation from a sealed tube operated at a 40 kV voltage and a 25 mA current and was calibrated with a standard silicon sample. The samples were scanned from $2\theta = 1$ to 30° at the step scan mode (step size 0.02°) at a scan rate of 1.2°/min, and the diffraction pattern was recorded using a proportional detector.

The Fourier Transform Infrared (FTIR) spectra of the samples were performed from a KBr pellet of the nanocomposites in a Thermo 5700 model instrument.

The Raman spectra of the solid samples were taken at the excitation wavelength of 780 nm using a Thermo Almega XR model.

The Ultraviolet-visible spectra (UV–Vis) of the P3OT and the SWCNT-P3OT composites were recorded using a UV–Vis spectrophotometer (Shimadzu Model UV–160) in a 1,2,4-trichlorobenzene solvent at room temperature from 200 to 800 nm.

The photoluminescence experiments of the polymer and the nanocomposite solutions were performed with a Hitachi instrument (FL-4500 fluorescence spectrometer). The photoexcitation was made at excitation wavelengths of 365, 450, and 465 nm.

For the FE-SEM study, a dried film of the polymer and composites was platinum coated and was observed through a Field Emission Scanning Electron Microscope (Hitachi S-4200) at 20 kV.

The dispersity of carbon nanotubes in the polymer matrix was studied using a Transmission Electron Microscope (TEM Hitachi, H-7100) operated at an accelerated voltage of 100 kV. A drop of diluted solution of the polymer/composite in ethanol dispersed by sonication on the carbon-coated copper grid was dried finally in a vacuum and was directly observed in the TEM.

The dc conductivity of P3OT and P3OT-SWCNT nanocomposite pellets were measured at room temperature using a Keithley/Luft semiconductor device analyzing system through I-V measurement.

RESULTS AND DISCUSSION

Characteristics of P3OT and P3OT/SWCNT composites (molecular weight)

The molecular weights determined through GPC are 53,490 (M_w) and 21,974 (M_n) for the polymer with 2.43 as a measure of polydispersity. The molecular

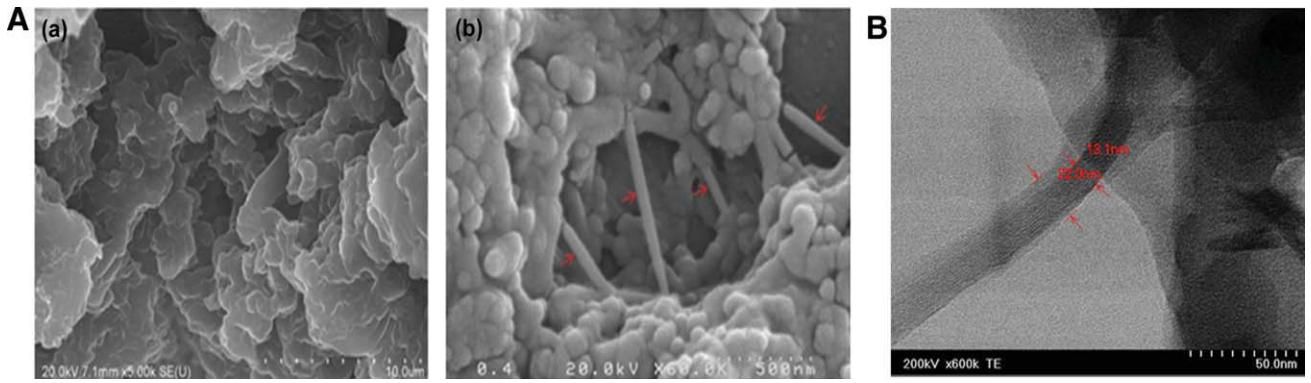

Figure 1 (A) SEM images of (a) P3OT and (b) P3OT/SWCNT (20%) composite. (B) TEM images of P3OT/SWCNT (20%) composite. [Color figure can be viewed in the online issue, which is available at www.interscience.wiley.com.]

weight of the polymer is noted to be in medium range, which will be useful for photovoltaic applications with easy processibility. It is reported that there is some slight variation in molecular weight with the extent of CNT loading in the case of composites.[21] This is quite possible considering the polymerization process to originate from the walls of the carbon nanotubes following heterogeneous nucleation process.

Morphology studies

A typical FE-SEM image of the P3OT and P3OT/SWCNT 20 wt % composite are presented in Figure 1A(a,b). By comparing them one can see the well-buried SWCNTs in the polymer matrix taking tubular structures. The TEM picture presented in Figure 1(B) presents a closer view of SWCNT with polymer wrappings.

Compositional analysis

Elemental analysis data of the polymer and 20% of the composite (Table I) show that there is a slight increase in the carbon content of the composite with a substantial decrease in the weights of sulfur and hydrogen, indicating the formation of the composites.

TABLE I
Elemental Analysis Data of SWCNT, P3OT, and P3OT/SWCNT Composite

Elements	SWCNT	P3OT	P3OT/SWCNT (20%)
C	97.53	73.45	79.98
S	1.90	16.91	12.80
H	0.29	9.64	7.08
N	0.29	0.00	0.14
Total	100	100	100

Structural elucidation

Fourier transform infrared spectra

The FTIR spectra of the SWCNT, P3OT, and P3OT-SWNT composites are shown in Figure 2. Theoretical investigation reveals that monocrystalling graphite belongs to the D^4_{6h} space-group symmetry[22] and the peak around 1562–1590 cm^{-1} are assigned with C=C stretch.[23,24] It is found at 1621 cm^{-1} in the as procured SWCNT sample as received. The further figures correspond to P3OT and its composites. In the case of P3OT the absorption bands 2918 and 2849 cm^{-1} correspond to —CH_2— stretch vibration and shoulder at 2952 cm^{-1} corresponds with the —CH_3 asymmetry stretch vibration. The bands centered at 1454 and 1370 cm^{-1} can be attributed to the bending vibration mode of —CH_2— and —CH_3. The characteristic in-plane and out-of-plane rocking vibration of —$(CH_2)_n$— group ($n \geq 4$) can also be observed at 719 and 1146 cm^{-1} in this spectra. For

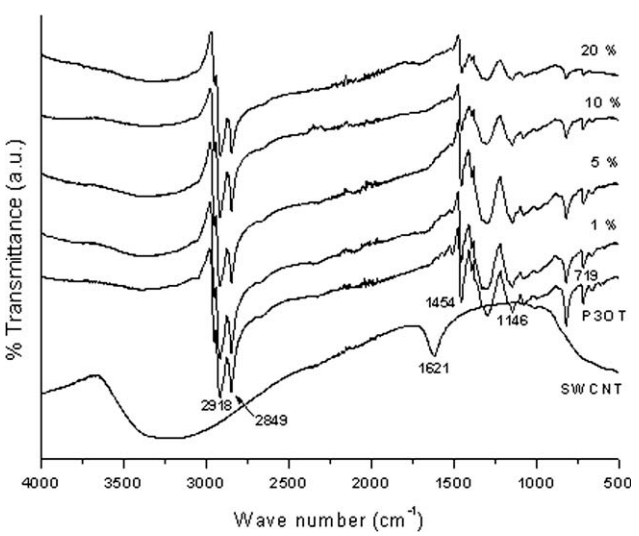

Figure 2 FTIR spectra of P3OT and P3OT/SWCNT composites.

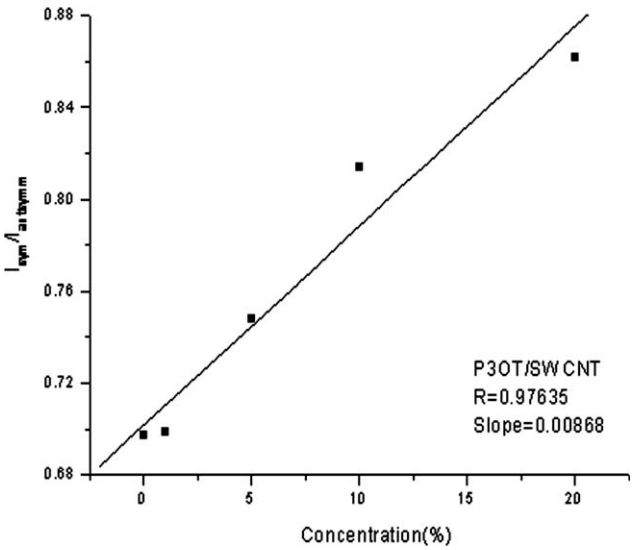

Figure 3 The intensity ratio of $I\nu_{antisymm}$ (C=C) /$I\nu_{sym}$ (C=C) Vs wt % of SWCNT.

P3OT there is no observation of the split of 719 cm^{-1} band into 720 and 730 cm^{-1}, which are representative of the ordered and disordered —CH_2— groups rocking vibration band.[25] According to Furukawa et al.[26] and Trznadel et al.[27] the ratio between the intensity of the antisymmetric C=C stretching peak (mode at 1510 cm^{-1}) and the intensity of the symmetric stretching peak (mode at 1456 cm^{-1}) can be used to probe the average conjugation length of P3HT. The same type of observation has been reported by Musumeci et al.[28] in their work of P3HT/MWNT composites. In this case there is no change in the ν_{sym}(C=C) and $\nu_{antisym}$(C=C) frequencies of the P3OT with successive loading of carbon nanotubes suggesting that there is no significant ground state interaction between the polymer and the CNT. The intensity ratio of $I\nu_{antisymm}$ (C=C)/ $I\nu_{sym}$ (C=C) Vs wt % of SWCNT is showing only a slight increment per unit addition of carbon nanotubes (slope in Fig. 3) and the 1450 cm^{-1} and 1510 cm^{-1} corresponding to stretch vibration of the thiophene ring has also not shown any tangible shift as claimed.[21] Hence it is not possible to think of any strong interaction between the carbon nanotube and the polymer, expect for some week π - π ground state interaction between the moieties.

Raman spectra

As Raman spectroscopy is sensitive to both electronic and vibrational structures of carbon nanotubes, it can be conveniently used to probe the structure of polymer nanocomposites. The spectra of SWCNT, polymer and the polymer composites are shown in Figure 4. In the signals of SWCNT, the important peaks at 1300 and 1590 cm^{-1} represent the sp^3 mode (D band) and the tangential mode (G band) of the nanotubes, respectively.[29] The intensity ratio of the D over G band (D/G ratio) has been used to predict the extent of purity of the nanotubes as well. With polymer-SWCNT composites the shift of G and D band frequencies is seen as a direct consequence of interaction between carbon tubes and the polymer. Wise et al.[30] have reported the effect as of an electron donor-acceptor type. Specifically, the charge removal from SWCNT results in an up shifting in the G band and a down shift in the Raman D band which is attributed to additional electron density in the SWCNT antibonding orbitals from charge injection. The Raman spectra recorded in the lower frequency part (RBM) has also been used to predict the inner diameter for the composites from lower frequency shifts.[31] The frequency position of the thiophene ring mode at about 1460 cm^{-1} has been observed to depend on the conjugation of the poly(alkylthiophene)s, being sensitive to deviation from the coplanarity of the chain segments.[32] In this study, the frequency of the G band has not shown any tangible shift and is centered on 1590 cm^{-1} suggesting that the polymer has not entered into any charge transfer with the nanotubes. Otherwise, the presence of SWCNT in the composites is very clear with higher concentrations of SWCNTs.

^{1}H-NMR spectra

The ^{1}H-NMR of the polymer and 20 wt % composite are presented in Figure 5(a,b). The P3OT spectrum is very well reproduced as in the literature for all the distinct protons.[33] But the proton signals of the terminal —CH_3, —CH_2— of the alkyl chain and the ring

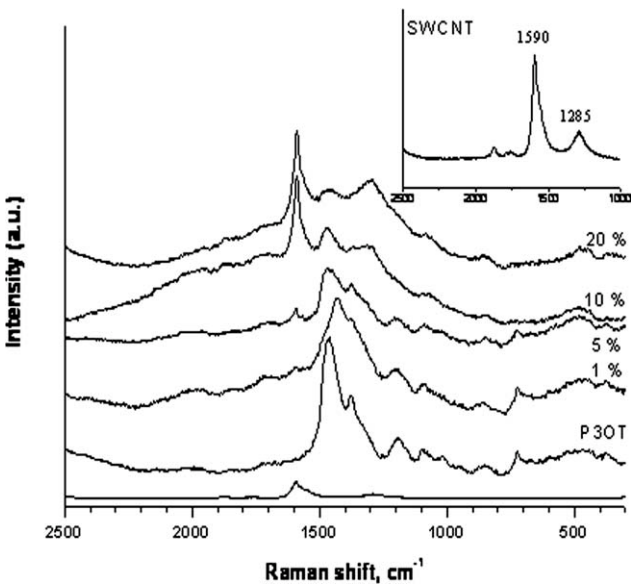

Figure 4 Raman spectra of P3OT, SWCNT, and P3OT/ SWCNT composites.

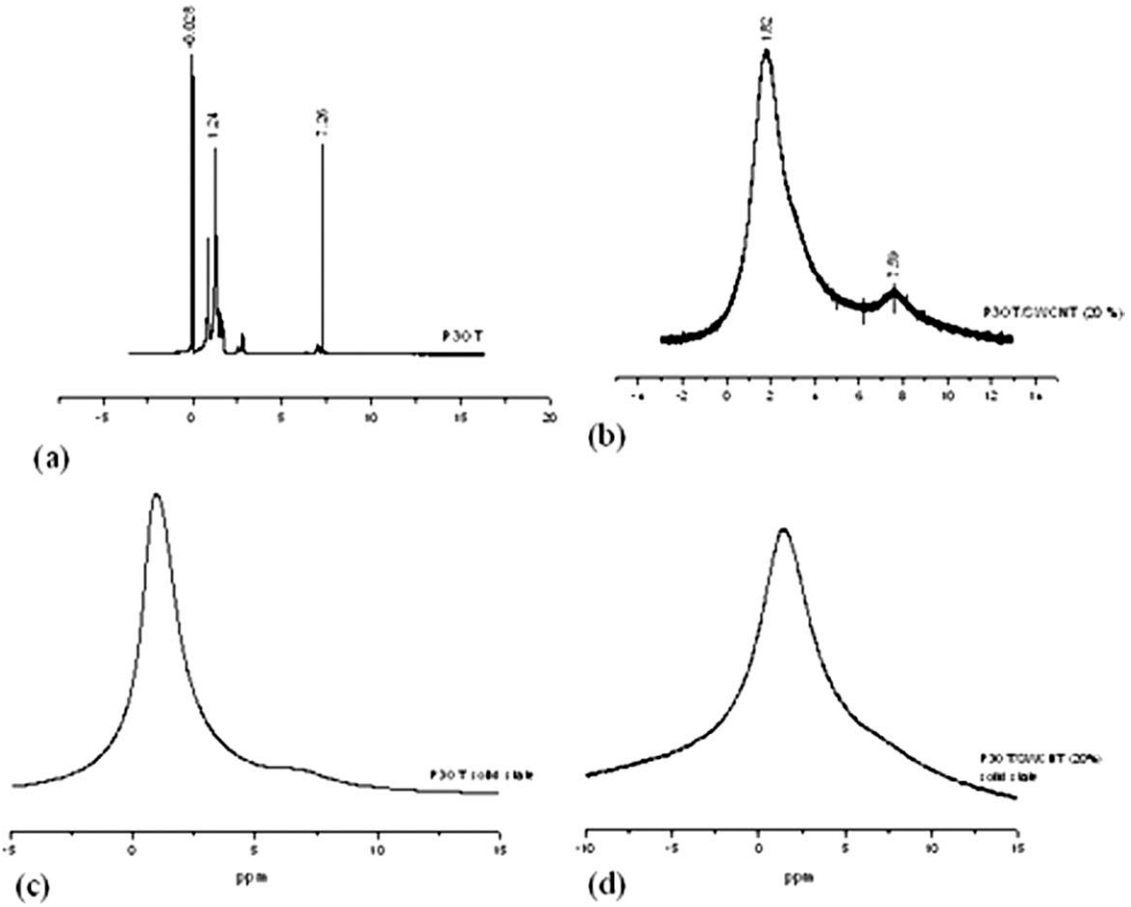

Figure 5 ^{1}H-NMR spectra (a) P3OT and (b) P3OT/SWCNT (20%) composite in $CDCl_3$, (c) P3OT, and (d) P3OT/SWCNT (20%) in solid form.

protons indicative of good regioregularity that lie between 0.88–2.803 ppm have also merged into a single broad peak appearing at 1.62 ppm and the 4th position ring proton of the thiophene ring that appears at 6.968 ppm for the polymer has broadened and then shifted for the composite. A possible explanation is that the polymer is being wrapped around the SWCNT, which are large species of low mobility.[34] This view is further strengthened when the solid state ^{1}H-NMR is examined for polymer and composite [Fig. 5(c,d)] where the individual proton peaks of the alkyl chain have merged into a single broad peak and shifted in position.

X-ray scattering

The X-ray diffraction patterns obtained at room temperature are shown in Figure 6. The scattering peaks at 4.06, 8.25, 12.53, and 23.9, 2θ arise from the first and higher order reflections from large length *d*-spacing (21.71 A°) for P3OT[32,35,36] and correspond to the in-plane interchain distance. Besides, an amorphous halo wide-angle peak with lesser intensity appears at 23.86° 2θ, *d*-spacing 4.06 A°, which represents the stacking distance of the thiophene rings or interplanar distance. There is no significant change in the scattering peaks' positions with the addition of SWNT with respect to interplane and intrachain distances. However the full-width at half-maximum (FWHM) suggests some changes in the crystallite size values (Table II). This could be due to the physical wrapping of the polymer on the walls of the nanotubes. This has been also interpreted as the composite showing a smaller large range order but a higher conformational order in the case of MWNT/P3HT composite with nanofiller present in high concentration.[28] The layered structure, with maximum chains forming parallel planes and side chains acting as spacers, is typical for a comb-like polymer in general indexed as (h00) (h.1,2,3, . . .)[37,38] and the corresponding *d*-spacing values can well imply the spacing between adjacent back bone chains.[39] With increased CNT loading, from 5% weight on wards the C(002) indicative of the graphite structure of short-SWCNTs in the composites could be observed.[40,41]

Work function

The work function is one of the most important physical quantities for their applications involving

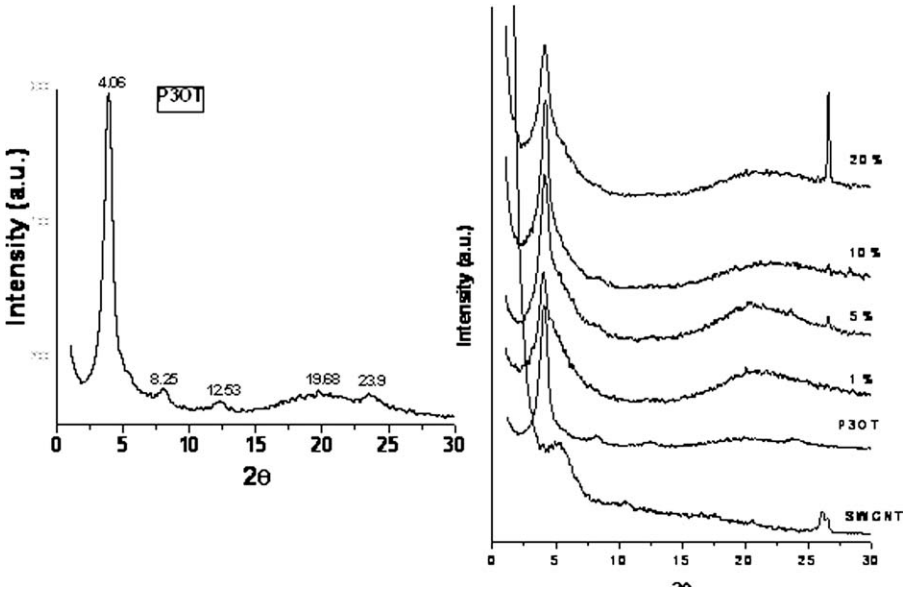

Figure 6 X-ray diffraction of SWCNT, P3OT, and P3OT/SWCNT composites.

electric contact between any metal electrode/conducting polymer and SWCNT. The values measured for SWCNT, P3OT, and P3OT/SWCNT (20% w/w) using photoelectron emission method are 4.92, 4.88 and 4.92 eV, respectively. It is known that the electronic structure of SWCNT strongly depends on their diameter and chirality.[42] The work functions of 93 SWCNTs are examined and found to be distributed in the range of 0.6 eV. However, most ranged in a small window of 0.2 eV. The variations are attributed to some bundle formations rather than to diameter dependence and differences between semiconducting and metallic SWCNT.[43] The value reported in this work is in the range previously reported.[44] As there is no significant variation in the values between polymer and composite, it may be inferred to indicate the absence of any tangible ground state interaction between the polymer and the nanotubes.

Optical properties

UV–Vis absorption spectra

The UV–Vis absorption spectra of P3OT and P3OT/SWCNT composites in 1,2,4-trichlorobenzene are presented in Figure 7. It is known that SWCNT absorption makes no significant contributions to the spectra.[45] The value of λ_{max} of P3OT (435 nm) is in line with an already reported value in the literature.[46] There is no significant shift in the λ_{max} of the polymer upon inclusion of carbon nanotubes in the form of composites. This suggests the lack of any ground state interaction and hence no appreciable charge transfer between the polymer and the SWCNT. Such observations have been reported in the case of P3OT/SWCNT blend composites[47] and also in the work of Nogueira et al.[31] The band gap values measured from optical absorbance results for the polymer and composites are around 2.36 ± 0.06 eV.

TABLE II
XRD Data of P3OT and P3OT/SWCNT Composite

System	d_1 (2θ)	d_2 (2θ)	Crystallite size (A°)
P3OT	21.7 (4.06)	3.72 (23.62)	125
SWCNT (1%)	22.12 (3.98)	3.52 (23.47)	197
SWCNT (5%)	21.56 (4.09)	3.72 (23.94)	125
SWCNT (10%)	20.82 (4.24)	3.35 (26.56)	174
SWCNT (20%)	21.69 (4.07)	3.35 (26.54)	169

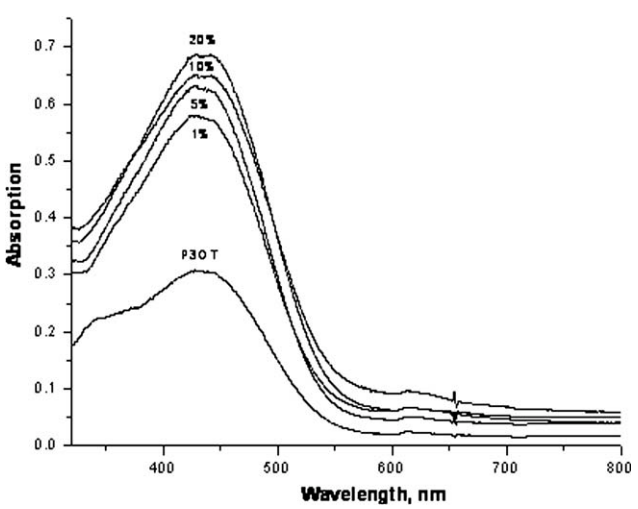

Figure 7 UV–Vis absorption spectra of P3OT and P3OT/SWCNT nanocomposites in $C_6H_3Cl_3$ solution at room temperature.

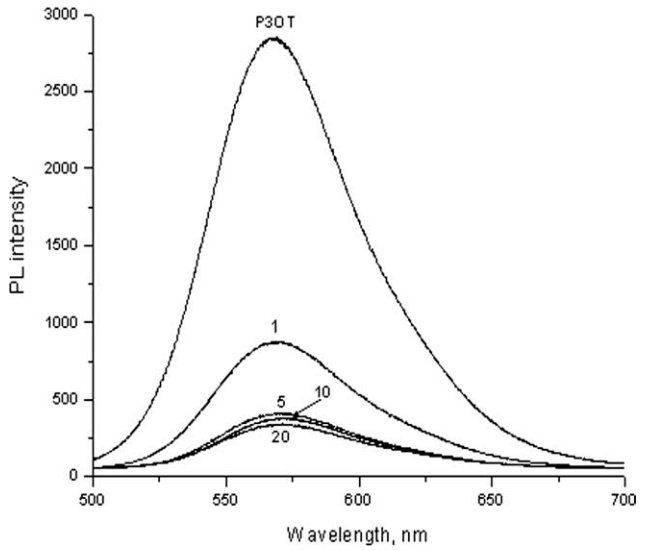

Figure 8 Photoluminescence spectra of P3OT and P3OT/SWCNT nanocomposites in $C_6H_3Cl_3$ solution at excitation 450 nm.

Photoluminescence spectra

The PL spectra of P3OT and its composites in 1,2,4-trichlorobenzene ($C_6H_3Cl_3$) for an excitations wavelength of 450 nm are presented in Figure 8. The other two excitation (365 and 465 nm) results are also indicative of the same trend. The polymer and the composites P3OT-1, P3OT-5, P3OT-10, and P3OT-20 show emissions in the range 567–570 nm. The reason for the photoluminescence quenching of the composites may be attributed to π-π interactions of P3OT with the nanotubes[48] forming additional decaying paths of the excited electrons through the SWCNT and the greater the concentration of the SWCNTs, the larger is the photoluminescence quenching. This larger quenching indicates the singlet exitons generated in the polymer are diminished before radiative recombination due to the presence of SWCNT in addition to absorption and scattering by the nanotubes. Furthermore in this case, the SWCNT acts as a nanometric heat sink which dissipates the heat generated from the incident beam.[49] The absence of any significant shift of the maximal luminescence peaks for the composites, at different excitation wavelength suggests extended molecular packing between the polymer and SWCNT to be of a physical nature and the absence of any important configurational relaxation in the excited state.[50]

Transport property-Conductivity

The electrical conductivity of conducting polymers depends on the extent of conjugation and the amount of dopant present in them.[51] Further in the case of polymer/CNT composites, it depends on the purity of the nanotubes and their alignments.[52] The DC electrical conductivity results of P3OT and its composites are presented in Table III. The conductivity of the polymer and its composites are measured using approximately 0.04 g of the samples, pressed into pellet form of 1.2 cm in diameter and 0.556 mm thickness using 600 kgf/cm^2 pressure by a manual hydraulic press for 15 min. The conductivity of P3OT at room temperature (20°C) is noted to be 4.2×10^{-9} S/cm. The conductivity of the polymer is increased with successive loading of the SWCNT in the limits of 1–20 wt % and reaches a maximum value of 4.74×10^{-4} S/cm, and a five fold increase. Critical masses below 1 wt % and frequently in the range of 0.01–0.1 wt % are reported for polymer/MWCNT composites.[53,54] A low percolation threshold indicates the efficient interaction between the nanotube and the polymer. Higher values are due to a lack of efficient debundling and isotropic dispersion in the polymer matrix. In the present case with the as-procured SWCNT, the percolation threshold from DC conductivity measurements is noted to be p_c= 0.5 wt % and $t = 3.19$, following model conductivity in the form $\sigma = \sigma_0(p\text{-}p_c)^t$ for $p > p_c$ (Fig. 9). A value of 2.7–3.2 for the exponent is reported for SWCNTs samples of different sources in the epoxy matrix.[41,55] Some of the individual CNTs or nanotube clusters isolated by polymer coatings are responsible for hoping transfer of electrons besides their tunneling through the nanotubes for a three dimensional percolation system.[56]

Dispersibility behavior

P3OT/SWCNT *in situ* polymerized composites exhibit good dispersibility in $CHCl_3$, THF, chlorobenzene etc. solvents much better than the simple blend of the polymer and SWCNT prepared through the sonication process. The hydrophobisity of the nanotubes are much reduced through the good wrapping of the polymer on the walls of the nanotube leading to a long stability of the solution and a much better dispersibility also. Both of the composites have been exhibited stability over 10 weeks, while the blend is stable for not more than 7 days. This will really be

TABLE III
DC Conductivity Data of SWCNT, P3OT, and P3OT/SWCNT Composite

Samples	P3OT	1% SWCNT	5% SWCNT	10% SWCNT	15% SWCNT	20% SWCNT
Conductivity, S/cm	4.2×10^{-9}	1.13×10^{-8}	5.44×10^{-6}	1.95×10^{-5}	2.6×10^{-4}	4.74×10^{-4}

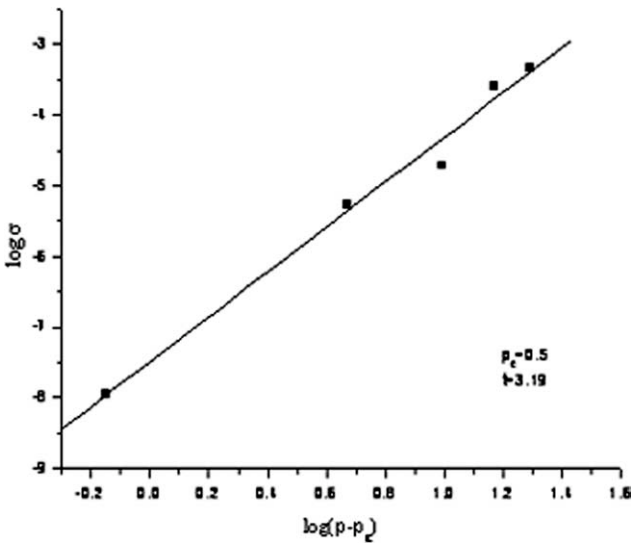

Figure 9 Plot of logσ vs. log(p-p_c) P3OT/SWCNT composites at room temperature.

an advantage while casting solar active coatings over a larger area substrate on a scaled-up level in field trials.

CONCLUSION

P3OT/SWCNT composite could be synthesized through *in situ* polymerization procedure using $FeCl_3$ oxidant. The lack of any significant ground state interaction involving any charge transfer, but only π-π stacking of noncovalent interaction type between the polymer and the walls of the nanotube is evident from FTIR, Raman, UV–Vis, PL spectra, and other measurements. ^{1}H-NMR also confirms the wrapping of the polymer on to the SWCNT indicating lack of mobility. The work function values and the optical band gap values measured also support this view. The *in situ* polymerization procedure of the donor polymer molecules and the acceptor carbon nanotubes has resulted in enhanced dispersibility and stability of the composites in organic solvents compared to the simple sonication of them providing convenient and reliable approach for their use in solar cell applications.

M. R. Karim gratefully acknowledges supports from King Saud University and Ministry of Higher Education, Kingdom of Saudi Arabia.

References

1. Yu, G.; Gao, J.; Hummelen, J. C.; Wudl, F.; Heeger, A. J. Science 1995, 270, 1789.
2. Campos, L. M.; Tontcheva, A.; Gunes, S.; Sonmez, G.; Neugebauer, H.; Sariciftci, N. S.; Wudl, F. Chem Mater 2005, 17, 4031.
3. Huynh, W. U.; Dittmer, J. J.; Alivisatos, A. P. Science 2002, 295, 2425.
4. Liu, J.; Tanaka, T.; Sivula, K.; Alivisatos, A. P.; Frechet, J. M. J Am Chem Soc 2004, 126, 6550.
5. Kymakis, E.; Amaratunga, G. A. J Appl Phys Lett 2002, 80, 112.
6. Kymakis, E.; Alexandrou, I.; Amaratunga, G. A. J. J Appl Phys 2003, 93, 1764.
7. Landi, B. J.; Raffaelle, R. P.; Castro, S. L.; Bailey, S. G. Prog PhotoVolt Res Appl 2005, 13, 165.
8. Landia, B. J.; Castrob, S. L.; Rufa, H. J.; Evansa, C. M.; Baileyc, S. G.; Raffaelle, R. P. Sol Energy Mater Sol Cells 2005, 87, 733.
9. Alam, M. M.; Jenekhe, S. A. Chem Mater 2004, 16, 4647.
10. Kietzke, T.; Horhold, H.-H.; Neher, D. Chem Mater 2005, 17, 6532.
11. Manoj, A. G.; Alagiriswamy, A. A.; Narayan, K. S. Appl Phys Lett 2003, 94, 4088.
12. Geng, J.; Zeng, T. J Am Chem Soc 2006, 128, 16827.
13. Karim, M. R.; Lee, C. J.; Park, Y.–T.; Lee, M. S. Synth Met 2005, 151, 131.
14. Shaffer, M. S. P.; Koziol, K. Chem Commun 2002, 2074.
15. Karim, M. R.; Yeum, J. H.; Lee, M. S.; Lim, K. T. Mater Chem Phys 2008, 112, 779.
16. Liu, I.-C.; Huang, H.-M.; Chang, C.-Y.; Tsai, H.-C.; Hsu, C.-H.; Tsiang, R. C.-C. Macromolecules 2004, 37, 283.
17. Karim, M. R.; Lee, C. J.; Chowdhury, A. M. S.; Nahar, N.; Lee, M. S. Mater Lett 2007, 61, 1688.
18. Kong, H.; Gao, C.; Yan, D. J Am Chem Soc 2004, 126, 412.
19. Zhao, B.; Hu, H.; Haddon, R. C. Adv Funct Mater 2004, 14, 71.
20. Karim, M. R.; Lee, C. J.; Lee, M. S. J Polym Sci Part A: Polym Chem 2006, 44, 5283.
21. Kuila, B. K.; Malik, S.; Batabyal, S. K.; Nandi, A. K. Macromolecules 2007, 40, 278.
22. Zhang, J.; Hongling, Z.; Qing, Q.; Yang, Y.; Li, Q.; Liu, Z.; Guo, X.; Du, Z. J Phys Chem B 2003, 107, 3712.
23. Li, X.; Zhang, J.; Li, Q.; Li, H.; Liu, Z. Carbon 2003, 41, 579.
24. Yu, X.; Rajamani, R.; Stelson, K. A.; Cui, T. Surf Coat Technol 2008, 202, 2002.
25. Qiao, X.; Wang, X.; Mo, Z. Synth Met 2001, 118, 89.
26. Furukawa, Y.; Akimoto, M.; Harada, I. Synth Met 1987, 18, 151.
27. Trznadel, M.; Pron, A.; Zagorska, M.; Chrzaszcz, R.; Pielichowski, J. Macromolecules 1998, 31, 5051.
28. Musumeci, A. W.; Glaura, G. S.; Liu, J.-W.; Martens, W. N.; Waclawik, E. R. Polymer 2007, 48, 1667.
29. Liu, Y. L.; Chen, W. H. Macromolecules 2007, 40, 8881.
30. Wise, K. E.; Park, C.; Siochi, E. J.; Harrison, J. S. Chem Phys Lett 2004, 391, 207.
31. Nogueira, A. F.; Lomba, B. S.; Soto-Oviedo, M. A.; Correia, C. R. D.; Corio, P.; Furtado, C. A.; Hümmelgen, I. A. J Phys Chem C 2007, 111, 18431.
32. Bolognesi, A.; Porzio, W.; Provasoli, A.; Botta, C.; Comotti, A.; Sozzani, P.; Simonutti, R. Macromol Chem Phys 2001, 202, 2586.
33. Fu, C.; Meng, L.; Lu, Q.; Zhang, X.; Gao, C. Macromol Rapid Commun 2007, 28, 2180.
34. Huang, W.; Fernando, S.; Allard, L. F.; Sun, Y.-P. Nano Lett 2003, 6, 843.
35. Chen, S. A.; Ni, J. M. Macromolecules 1992, 25, 6081.
36. Shiga, T.; Okada, A. J Appl Polym Sci 1996, 62, 903.
37. Tashiro, K.; Ono, K.; Minagawa, Y.; Kobayashi, M.; Kawai, T.; Yoshino, K. J Polym Sci Part B: Polym Phys 1991, 29, 1223.
38. Mardalen, J.; Samuelsen, E. J.; Gautun, O. R.; Carlsen, P. H. Solid State Commun 1991, 77, 337.
39. Hsu, W. P.; Levon, K.; Ho, K. S.; Myerson, A. S.; Kwei, T. K. Macromolecules 1993, 26, 1318.
40. Andrews, R.; Jacques, D.; Qian, D.; Dickey, E. C. Carbon 2001, 39, 1681.
41. Huang, Y.; Li., N.; Ma, Y.; Du, F.; Li, F.; He, X.; Lin, X.; Gao, H.; Chen, Y. Carbon 2007, 45, 1614.

42. Saito, R.; Dresselhaus, G.; Dresselhaus, M. S. Physical Properties of Carbon Nanotubes; Imperial College Press: London, 1998.
43. Suzuki, S.; Watanabe, Y.; Homma, Y.; Fukuba, S.; Heun, S.; Locatelli, A. Appl Phys Lett 2004, 85, 127.
44. Shiraishi, M.; Ata, M. Carbon 2001, 39, 1913.
45. Ovsyannikova, E. V.; Efimov, O. N.; Moravsky, A. P.; Loutfy, R. O.; Krinichnaya, E. P.; Alpatova, N. M. Russ J Electrochem 2005, 41, 439.
46. Babel, A.; Jenekhe, S. A. Synth Met 2005, 148, 169.
47. Kymakis, E.; Amaratunga, G. A. J. Synth Met 2004, 142, 161.
48. Chen, J.; Liu, H.; Weimer, W. A.; Halls, M. D.; Waldeck, D. H.; Walker, G. C. J Am Chem Soc 2002, 124, 9034.
49. Feng, W.; Fujii, A.; Ozaki, M.; Yoshino, K. Carbon 2005, 43, 2501.
50. Colladet, K.; Fourier, S.; Cleij, T. J.; Lutsen, L.; Gelan, J.; Vanderzande, D.; Nguyen, L. H.; Neugebauer, H.; Sariciftci, S.; Aguirre, A.; Janssen, G.; Goovaerts, E. Macromolecules 2007, 40, 65.
51. Mohammad, F.; Calvert, P. D.; Billingham, N. C. J Phys D: Appl Phys 1996, 29, 195.
52. Peng, H. J Am Chem Soc 2008, 130, 42.
53. Gojny, F. H.; Wichmann, M. H. G.; Fiedler, B.; Kinloch, I. A.; Bauhofer, W.; Windle, A. H.; Schulte, K. Polymer 2006, 47, 2036.
54. Kim, Y. J.; Shin, T. S.; Choi, H. D.; Kwon, J. H.; Chung, Y. C.; Yoon, H. G. Carbon 2005, 43, 23.
55. Bryning, M. B.; Islam, M. F.; Kikkawa, J. M.; Yodh, A. G. Adv Mater 2005, 17, 1186.
56. Barrau, S.; Demont, P.; Peigney, A.; Laurent, C.; Lacabanne, C. Macromolecules 2003, 36, 5187.